43rd AIAA/ASME/SAE/ASEE Joint Propulsion Conference & Exhibit
8 - 11 July 2007, Cincinnati, OH



43rd AIAA/ASME/SAE/ASEE Joint Propulsion Conference and Exhibit
Cincinnati, OH, July 8-11, 2007 AIAA 2007-5406

# Performance of Supersonic Model Combustors with Distributed Injection of Supercritical Kerosene

**X. J. Fan[*], G. Yu[†], J. G. Li[‡], and X. N. Lu[§]**
*Chinese Academy of Sciences, Beijing, 100080, P. R. China*

and
**C. J. Sung[£]**
Case Western Reserve University, Cleveland, OH 44106, USA



## Abstract

Supersonic model combustors with two-staged injections of supercritical kerosene were experimentally investigated in both Mach 2.5 and 3.0 facilities with the stagnation temperatures of approximately 1750K. Supercritical kerosene at temperatures of approximately 760K and various pressures was prepared using a two-staged heater developed in Ref. 1 and injected at equivalence ratios of 0.98 to 1.46. Two pairs of integrated injector/ flameholder cavity models in tandem were used to facilitate the fuel-air mixing and stabilize the combustion. Combustor performances with different fuel injection locations, injector numbers, combinations of injection stages, and combustor entry Mach numbers were investigated systematically and discussed based on the measured static pressure distributions and the specific thrust increments due to combustion. With two-staged fuel injections the overall performance of the combustors was shown to be improved and fuel injections at equivalence ratio higher than unity could be reached without combustor-inlet interaction. Reducing the number of injectors while increased its diameter was very effective to increase the pressure rise in the combustor with single-stage injections but had little effect on the combustor performance with two-staged fuel injections. Increasing the entry Mach number resulted in lower combustion levels, in particular, with fuel injections at locations close to the combustor exit but was balanced with two-staged fuel injections.

## Introduction

In hydrocarbon-fueled scramjet operations, the onboard fuel will be also used as a coolant and its temperature and state will vary with the different flight stages. When both fuel temperature and pressure are higher than the thermodynamic critical point, the fuel becomes supercritical. Supercritical fuel exhibits liquid-like density and gas-like diffusivity.[1] During injection the supercritical fuel can be directly transformed to the gaseous state without atomization and vaporization processes. Our previous experimental investigation[2] demonstrated that the use of supercritical kerosene injection holds the potential of enhancing fuel-air mixing and promoting overall burning and in comparison with liquid fuel injections at similar fuel flow rates, the pressure rises in the combustor with supercritical fuel injections could be increased significantly at relatively lean conditions (equivalence ratios blow approximately 0.5 for the tested Mach 2.5 combustor). However, further increase in the fuel flow rate and the pressure rise with the single-stage injection was limited by the upstream propagation of boundary layer separation due to excessive heat release.[3] Thus, the advantage of supercritical fuel injection has not been fully accomplished with single-stage injection.

A longer isolator or a further downstream injection location could be used to suppress upstream propagation of the boundary layer separation. However, a longer isolator may cause an increase in drag and engine weight, while moving the injection to a further downstream location may cause an decrease in combustion efficiency and lower pressure rise due to poor jet penetration and the shorter fuel residence time. The idea of staged fuel injection4[4] utilizes the combustion of an upstream-injected fuel to improve the mixing and burning processes of the downstream-injected fuel, while still keep the fuel flow rate through the upstream injectors below the allowable value. In this case, better pressure distributions and higher thrust could be attained.[5-7]

On the other hand, in a practical scramjet operation, it is also advantageous to use fuel distributions to adjust the fuel delivery with different flight conditions and achieve an optimum engine performance.

To further explore these ideas, a series of experiments were conducted to characterize the combustion of supercritical kerosene injected at two different stages in both Mach 2.5 and 3.0 model combustors. The fuel was injected through two pairs of integrated injector/ flameholder cavity models installed in tandem along the flow path. The distribution of supercritical kerosene was achieved using two sonic

[*] Associate Professor, Institute of Mechanics, 15 Beisihuanxi Road, Haidian District, xfan@imech.ac.cn, Member AIAA.
[†] Professor, Institute of Mechanics, yugong@imech.ac.cn, Member AIAA.
[‡] Professor, Institute of Mechanics, jgli@imech.ac.cn, Member AIAA.
[§] Professor, Institute of Mechanics, xnlu@imech.ac.cn.
[£] Professor, Department of Mechanical and Aerospace Engineering, cjs15@case.edu, Senior Member AIAA.

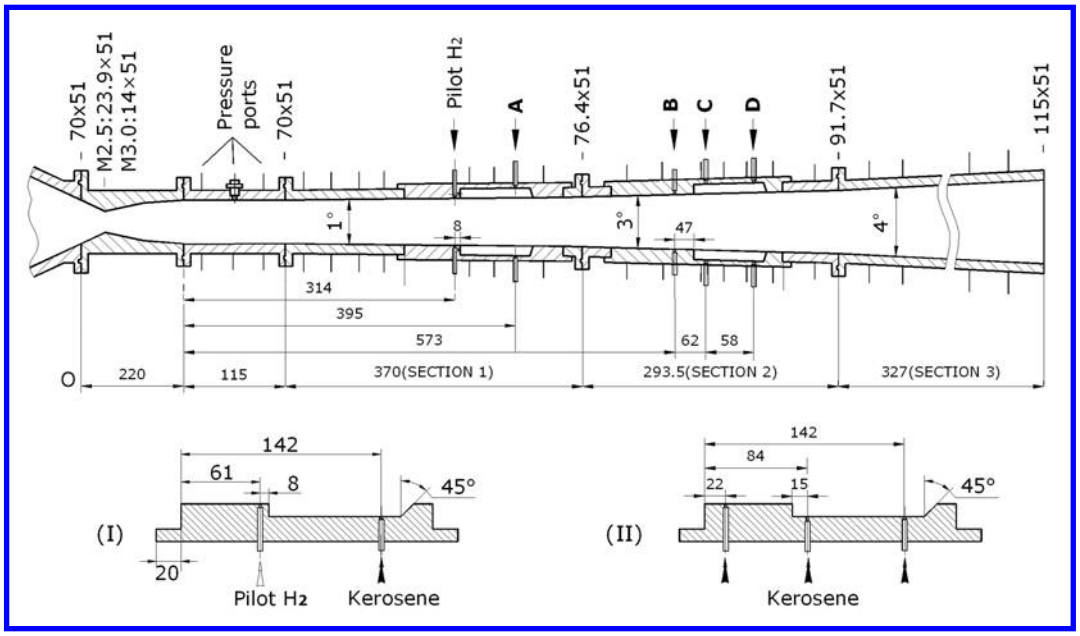


**Fig. 1 Schematic of Mach 2.5 and 3.0 model combustors (top) and integrated fuel injection and flameholder module (bottom). All dimensions are in mm.**

nozzles of different sizes. Emphases were placed on the effects of locations of the second-stage injections, the injector/cavity integrations, and different combinations of injector numbers and diameters on the combustor performance. The effects of combustor entry Mach numbers and pilot hydrogen were also examined.

## Experimental Specifications

*Test Facility*

The experiments were conducted in a direct-connect wind tunnel facility, which consisted of a vitiated air supply system, a multi-purpose supersonic model combustor, and a kerosene delivery and heating system. The facility operation, control, and data acquisition were accomplished with a computer. The vitiated air heater was used to supply heated airflow with a stagnation temperature ($T_0$) of 1750 ± 70 K. Two nozzles were used to accelerate the flow to Mach 2.5 or 3.0. The nozzle throat dimensions were 23.9 mm × 51 mm and 14.0 mm × 51 mm for Mach 2.5 and 3.0 flow, respectively. To keep the static pressure in the combustor almost identical, the stagnation pressures ($P_0$) of the airflow was set to 1.12 ± 0.02 and 2.44 ± 0.06 MPa for Mach 2.5 and 3.0 flow, respectively.

The model combustor shown in Fig. 1 had a total length of 1105.5 mm and consisted of one nearly constant area section of 115 mm and three divergent sections of 370, 293.5, and 327 mm with the expansion angles of 1, 3, and 4 degrees, respectively. The entry cross section of the combustor was 70 mm in height and 51 mm in width. In Fig. 1, the "0" indicated at the beginning of the constant area section represents the origin of all the static pressure distributions to be presented and discussed later.

Two pairs of interchangeable integrated fuel injector/flameholder cavity modules in tandem were installed on both sides of the combustor, each with a depth of 12 mm, a 45-degree aft ramp angle, and an overall length-to-depth ratio of 7.3. There were four rows of wall injectors for kerosene injection (designated as stage A-D in Fig. 1) installed on each sidewall and integrated to the cavity modules at streamwise locations of 395, 573, 635, and 693 mm. For each row of injectors, three injector configurations (orifice number × diameter) of 9 × 1.0 mm, 4 × 1.2 mm and 2 × 1.7 mm were used in the experiments. A small amount of pilot hydrogen was used to facilitate the self-ignition of kerosene in the supersonic combustor. There were five orifices of 1.0 mm in diameter available for pilot hydrogen injection. Room temperature pilot hydrogen was injected normally to the airflow just upstream of the first pair of cavities. The typical equivalence ratio of pilot hydrogen used in this study was 0.09.

Stagnation pressure and stagnation temperature of vitiated air ware measured using a CYB-10S pressure transducer and a Type B thermocouple, respectively. Static pressure distribution in the axial direction was determined using Motorola MPX2200 pressure transducers installed along the centerline of the model combustor sidewalls. The experimental uncertainty in the pressure and temperature measurements was approximately 3%.

The entire test rig was mounted upright on a platform. Three weight sensors (Shanghai TM, Model No. NS-TH3), equilaterally spaced and connected in series, were used to support the platform and measure the thrust changes during the experiments. This system yielded a maximum force reading of 7500 N with an uncertainty of 0.2%. Figure 2 shows a typical time history of the thrust signal for a single run. The airflow started up at the point "a". Subsequently, the thrust was seen to increase rapidly and level off within one second. Fuel injection then began at the point "b". The thrust level further increased due to the fuel injection and the subsequent supersonic combustion of fuel, and quickly stabilized at the point "c". After a certain experimental duration, the airflow and fuel injection were shut off at the point "d" and the thrust quickly dropped to the point "e". It is seen from Fig. 3 that the thrust increased very slightly from the point "c" to the point "d" because of the time required establishing thermal equilibrium between the core flow and the combustor walls. Nevertheless, the nearly constant thrust level between the points "c" and "d" demonstrates the steadiness of the resulting supersonic combustion and the adequacy of the present test facility. The thrust increment as a result of fuel injection and combustion is then defined as the thrust increase from the value at the point "b" to the average value between the points "c" and "d". This thrust increment will be later used as one target parameter for the combustor performance assessment.

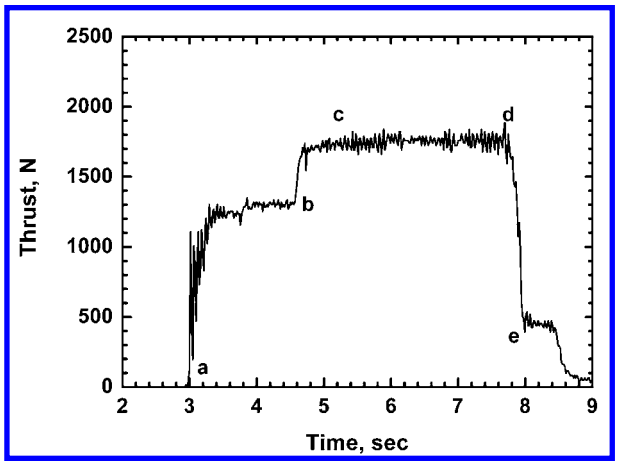


**Fig.2 Typical time history of thrust value during experiment.**

*Kerosene Delivery and Heating System*

Supercritical kerosene at temperature of 750 ± 20 K and various pressures was prepared using the two-stage kerosene heating and delivery system developed in Ref. 1. A schematic of the system is shown in Fig. 3. The first stage was a storage type heater that can heat kerosene of 0.8 kg up to 570 K in approximately 10 minutes with negligible coking deposits. The second stage heater was a continuous type, which was capable of rapidly heating kerosene to 750 K. The residence time of heated kerosene within the second-stage heater was typically less than 4 seconds, thereby minimizing the extent of fuel coking.

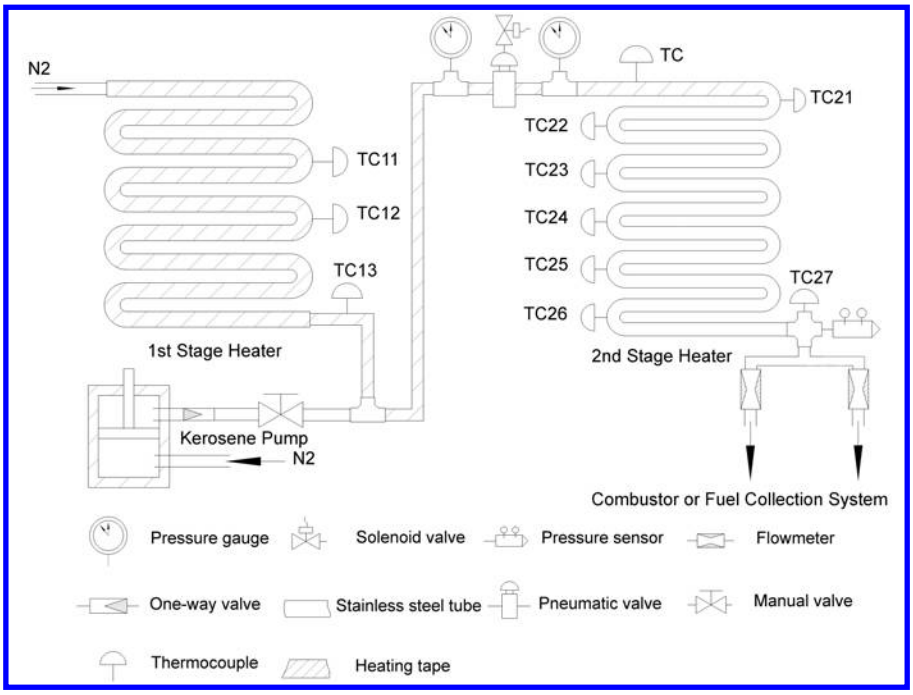


**Fig. 3 Schematic of kerosene delivery and heating system.**

Prior to each experiment the kerosene in a storage cylinder was pumped into the first-stage heater by a piston. Two pneumatic valves (Swagelok, Model No. SS6UM and SS10UM) installed respectively at the exits of the first- and second- stage heaters were employed to turn on/off the two heaters sequentially, as shown in Fig. 3. When kerosene in the first-stage heater reached a desired temperature at a given pressure, kerosene was pressed into the second-stage heater and heated up to the working temperature before injected into the combustor.

Two groups of K-type thermocouples (Omega, Model No. KMQSS-0.032E), TC11–13 and TC21–27 in Fig. 3, which were installed on the surface of or inserted into the heater tubes, were used to monitor and achieve the feedback control of fuel temperature distribution along the heating system. Stable fuel temperature and pressure at the exit of the heating system were accomplished and maintained during the experiments.

The mass flow rates of supercritical kerosene were controlled and measured by sonic nozzles and calibrated using the calibration method developed in our previous study.[1] In cases of fuel distribution, two sonic nozzles of different diameters were installed in parallel at the exit of the second stage heater. The mass flow rate of each sonic nozzle was determined by the fuel temperature and pressure measured just upstream the nozzles. Five different nozzle throat diameters of 1.60, 2.15, 2.5, 2.81, and 3.08 mm were employed to cover the flow rate range tested. Considering the measurement accuracies of throat area, fuel pressure, and fuel temperature, the overall uncertainty associated with the measured fuel mass flow rate was within 5%.

## Results and Discussion

*Effects of Injection Location*

Experiments were first conducted in the Mach 2.5 combustor under approximately identical flow conditions: a stagnation temperature of 1750 ± 70 K, a stagnation pressure of 1.12 ± 0.02 MPa and a mass flow rate of 1200 ± 20 g/s. Injector configuration of 9 × 1.0 mm was used for kerosene injection. The kerosene was injected at the supercritical conditions of 750 ± 20 K and 4.93 ± 0.03 MPa. The fuel mass flow rate was 114 ± 2 g/s, which corresponds to an equivalence ratio of 1.44 ± 0.02.

Figure 4 shows the static pressure distributions along the combustor with single-staged fuel injection at four different locations of A-D. The pressure distribution without fuel injection is also plotted as reference. Although the same amount of kerosene was injected at each location, the overall pressure rise with the stage-A injection was much higher than the other threes. The pressure rise with the stage-A injection was observed to commence even within the isolator section. As the injection moved to downstream locations, the overall pressure level decreased, the "pressure leg" into the isolator became shorter, but the pressure downstream of the second cavity increased. The pressure profiles with stage B-D injections were quite similar, and only one peaks observed at the second cavity location. There was some drastic changes occurred in the profile when fuel was injected at the location A. Its peak occurred at the first cavity location, but downstream the peak, the pressure decreasing in the divergent sections was divided by the second cavity into two parts each with different descent slopes.

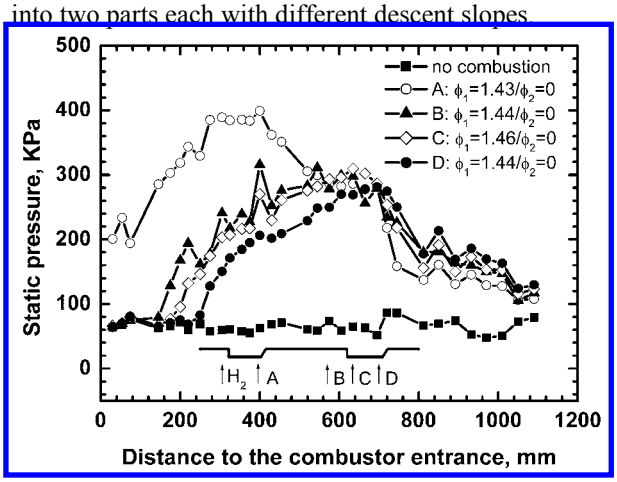


**Fig. 4 Comparison of static pressure distributions with single-staged fuel injection at different locations under identical fuel injection conditions. Vitiated Mach 2.5 air: $T_0$ ~ 1750 K and $P_0$ ~ 1.12 MPa.**

The measured thrust increments per unit mass flow rate of air ($\Gamma$) were listed Table 1 for the conditions in Fig. 4 and all other experiments conducted herein. The thrust increment decreased from 369 to 312 m/s when the injection location was moved from A to C. $\Gamma$ with the stage-D injection increased back to 343 m/s despite its pressure rise was much lower than others in the first half of the profile as shown in Fig. 4, which can be explained by the higher pressure rise downstream of the second cavity where the divergent angle was much steeper.

To void the pressure rise propagation back into isolator with the stage-A injection, the fuel flow rate was reduced to 57.5% of its initial value and the remaining 42.5% was injected through one of the three stages. Because the changes in the total area of sonic-nozzle flow meters for two-staged injections, the fuel injection pressure was reduced to 4.25 ± 0.07 MPa to keep the fuel flow rate almost identical. Figure 5 compares the static pressure profiles with the A+B, A+C and A+D injection combinations. Surprisingly, the pressure profiles for all three cases were nearly identical within the experimental uncertainty,

regardless of the differences in locations of the second stage injections or the fuel residence times. The difference in the thrust increments was also narrowed as shown in table 1. This feature was quite different from the test results in a supersonic combustor[7], probably due to different ratios of fuel flow rates. It might be true that the fuel-air mixing and the burning intensities of fuel injected at the downstream locations were improved by the lower flow Mach number and higher turbulence intensity resulted from the combustion of fuel injected at stage-A. Figure 5 also shows that the "pressure legs" into the isolator became much lower in comparison with the first profile in Fig. 4

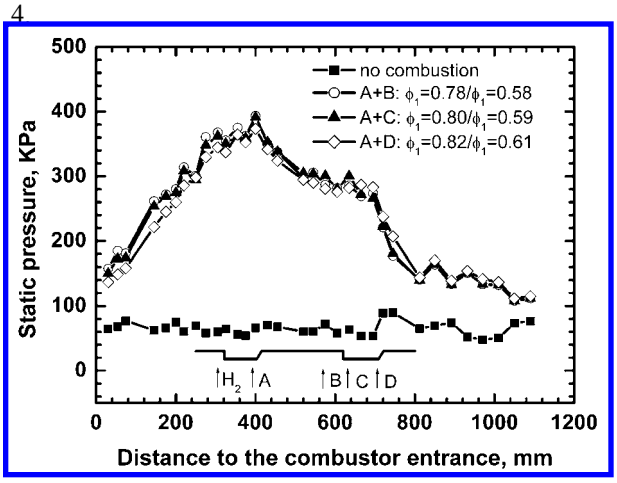


**Fig. 5 Comparison of static pressure distributions with two-staged fuel injections under identical fuel injection conditions. Vitiated Mach 2.5 air: $T_0$ ~ 1750 K and $P_0$ ~ 1.12 MPa.**

*Effects of injector configuration*

To examine the effects of different combinations of orifice numbers and diameters, combustion tests with the stage-B injections were conducted in the Mach 2.5 combustor. The airflow and kerosene injection conditions were kept approximately the same as that in Fig. 4. Three injector configurations (orifice number × diameter) of 9 × 1.0 mm, 4 × 1.2 mm and 2 × 1.7 mm were used in the experiments. Figure 6 compares the pressure distributions for the three configurations at almost identical fuel flow rates. It can be seen from Fig. 6 that the pressure level increased definitively as the injector number reduced and its diameter increased. With the same total fuel flow rate, less number or larger diameter of injectors corresponds to higher fuel flow rate through a single injector and accordingly, the penetration depth of fuel jet would be larger[7], resulting in higher fuel-air mixing level and combustion intensity. The thrust increment per unit mass flow rate of air in table 1 shows the similar tendency.

When two-staged injection was employed, the benefit of using larger-diameter injectors needs to be determined experimentally. Combustor performances with A+B fuel injections were examined as an example. Same injector configuration was used for stage-A and stage-B injections in each run. The airflow and kerosene injection conditions were kept approximately the same as that in Fig. 6. To suppress combustor-inlet interaction, only 42.5% of total fuel flow rate was injected through stage-A. Figure 7 compares the pressure distributions with A+B fuel injections for the above three injector configurations at almost identical total fuel flow rates. It can be seen that the difference in pressure rises due to different injector configurations became considerably smaller with two-staged injections. The difference in the thrust increment as shown in table 1 was also reduced.

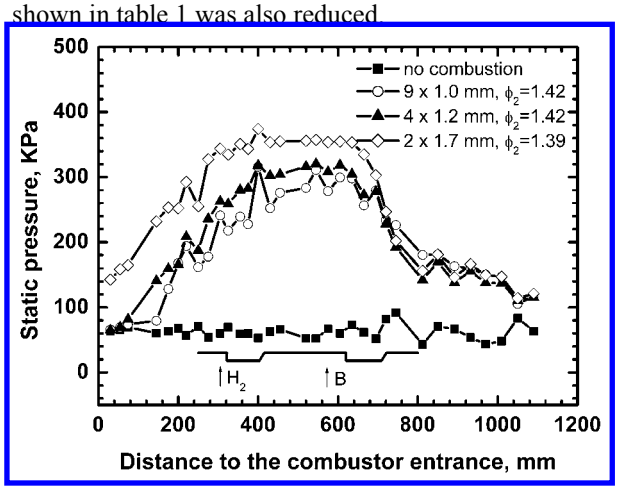


**Fig. 6 Comparison of static pressure distributions with different injector configurations under identical fuel injection conditions. Vitiated Mach 2.5 air: $T_0$ ~ 1750 K and $P_0$ ~ 1.12 MPa.**

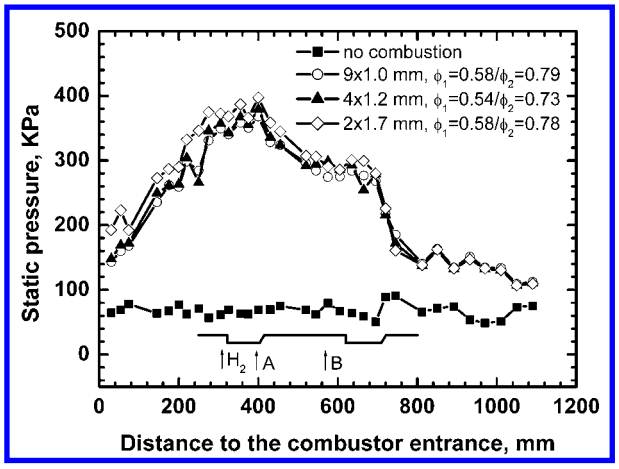


**Fig. 7 Comparison of static pressure distributions with stage A+B fuel injections for different injector configurations under identical fuel injection conditions. Vitiated Mach 2.5 air: $T_0$ ~ 1750 K and $P_0$ ~ 1.12 MPa.**

*Effects of Combustor Entry Mach Number*

The combustor entry Mach number plays important roles in affecting combustor performance. A higher entry Mach number might reduce the burning intensity due to shorter fuel residence time, particularly with fuel injections at locations closer to the combustor exit. To verify the effectiveness of staged injections in performance enhancement of a higher speed combustor, a series of experiments with single- and two- staged fuel injections were also carried out in the Mach 3.0 combustor under approximately identical flow conditions: a stagnation temperature of 1750 ± 70 K, a stagnation pressure of 2.45 ± 0.03 MPa and a mass flow rate of 1480 ± 20 g/s. Injector configuration of 9 × 1.0 mm was used for kerosene injection. The kerosene was injected at the supercritical conditions of 750 ± 20 K and 4.55 ± 0.03 MPa. The fuel mass flow rate was 103 ± 2 g/s, which corresponds to an equivalence ratio of 1.03 ± 0.03.

Figure 8 shows the static pressure distributions along the Mach 3.0 combustor with fuel injected at four different locations of A-D. In comparison with the Mach 2.5 test results in Fig. 4, similar tendencies in pressure level variations with different injection locations were observed in Fig. 8, except that there was more diversity in the pressure distributions with the stage B-D injections. Particularly very low burning intensity can be identified with the stage-D injection in which most of injected fuel left the combustor without combustion.

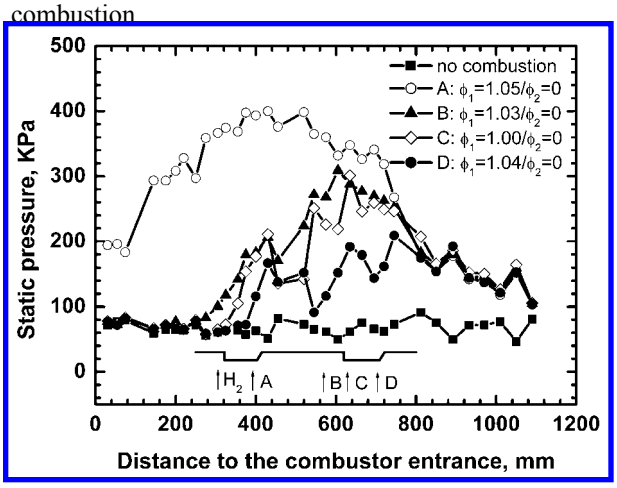


**Fig. 8 Comparison of static pressure distributions with single-staged fuel injection at different locations under identical fuel injection conditions. Vitiated Mach 3.0 air: $T_0$ ~ 1750 K and $P_0$ ~ 2.45 MPa.**

Figure 9 compares the static pressure profiles with the A+B, A+C and A+D injection combinations. The fuel injection pressure was reduced to 4.12 ± 0.02 MPa to keep the fuel flow rate almost identical to that in the single-staged injections. Approximately 42.5% of the total fuel flow rate was injected through stage-A and the remaining 57.5% was injected through one of the three stages B-D located at the second cavity module. Again, the pressure profiles and thrust values for all three cases were nearly the same except that a little more diversity existed compared to Fig. 5.

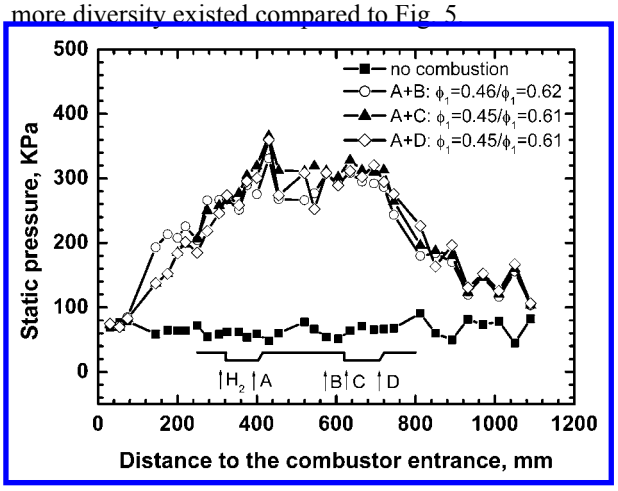


**Fig. 9 Comparison of static pressure distributions with two-staged fuel injections under identical fuel injection conditions. Vitiated Mach 3.0 air: $T_0$ ~ 1750 K and $P_0$ ~ 2.45 MPa.**

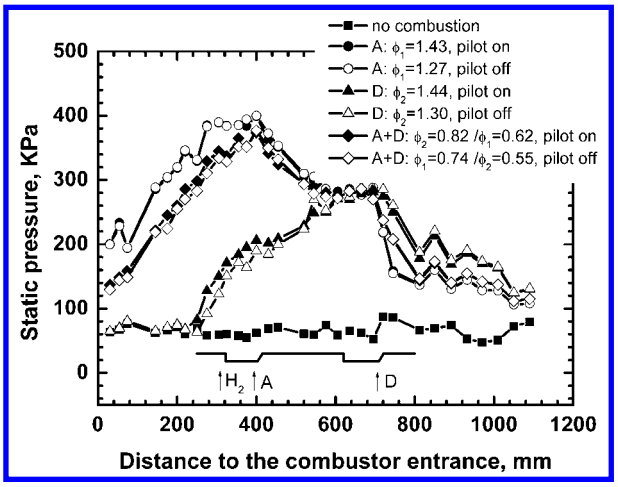


**Fig. 10 Comparison of static pressure distributions with and without pilot hydrogen injections. Vitiated Mach 2.5 air: $T_0$ ~ 1750 K and $P_0$ ~ 1.12 MPa.**

*Effects of Pilot Hydrogen*

The preceding results were obtained with the help of pilot hydrogen at relatively large equivalence ratio of 0.09. To clarify the role of pilot hydrogen played in the supersonic combustion with staged fuel injection, the pilot hydrogen during the experiments was turn off about one second earlier than the fuel. Thus comparisons of the combustor performances between pilot hydrogen turning on and off could be made. Figure 10 compares the pressure distributions in the Mach 2.5 combustor with fuel injection from stage-A, stage-D and stage A+D, with and without pilot

hydrogen injections. The airflow and fuel injection conditions were identical to these in Fig. 4 and Fig. 5 for single and staged injections, respectively. Note that there were same changes in fuel equivalence ratio when pilot hydrogen was cut off. It shows from Fig. 10 that, when pilot hydrogen was turned off, the pressure level was almost not affected with the stage-A injection, decreased a little with the stage-D injection, and only slightly with staged injection. However, stable combustions were maintained in all cases. Figure 10 also shows clearly that the pressure level with staged injections was much higher than that with the stage-D injection and little lower than that with stage-A injection. Mach 3.0 combustor showed similar effects of pilot hydrogen but the corresponding amplitudes of pressure drops were slightly larger than the Mach 2.5 combustor.

*Issues Related to the Fuel Jet Penetration depth*

For a sonic or supersonic jet discharging into a supersonic flow, its penetration depth is proportional roughly to the flow rate of gaseous jet and the square root of the static pressure ratio between the jet flow and the primary flow.[8] For a supercritical kerosene jet, sonic conditions could be also reached at the injector, and the above conclusion might be still applied. Figure 11 compares the pressure distribution along the Mach 2.5 combustor at different pressures but same flow rates and at similar pressures but different flow rates. The fuel was injected at stage-B. Figure 11 showed that the pressure level only varied slightly with a 27% increase in the injection pressure but increased significantly with a 37% increase in the fuel flow rate. Table 1 shows that the $\Gamma$ increased 21% with the increased flow rate.

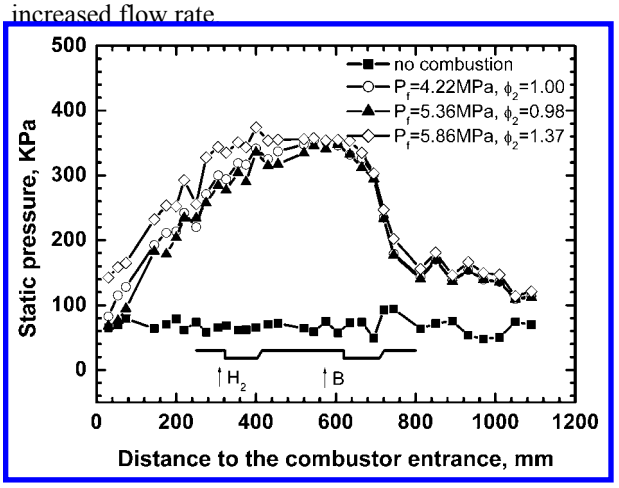


**Fig. 11 Comparison of static pressure distributions with different fuel pressures and flow rates. Vitiated Mach 2.5 air: $T_0$ ~ 1750 K and $P_0$ ~ 1.12 MPa.**

## Conclusions

Combustor performances with two-staged kerosene injections were experimentally investigated in both Mach 2.5 and 3.0 facilities with the stagnation temperature of approximately 1750K. Kerosene was injected under supercritical conditions through two pairs of integrated injector/ flameholder cavity models installed in tandem. Combustor performance was assessed using the static pressure distributions and the thrust increments during the experiments. The results were compared with that with single-staged injections at different injection locations. The following results were obtained.

Staged injection was very effective to improve the overall burning intensity regardless the locations of the second stage injections and to suppress the upstream propagation of boundary layer separation driven by pressure rise.

Reducing the number of injectors and increasing its diameter had little effect on the combustor performance with two-staged fuel injections, although it was very effective on that with single-stage injections.

Higher combustor entry Mach number is adversary to the mixing and combustion with single-staged fuel injections but only has little effect on the combustor performance with two-staged fuel injections.

## Acknowledgments

This research was supported by the Natural Science Foundation of China under contract no. 10672169. The authors would like to thank Mr. Ying Li and Mr. Xuesong Wei for their technical support during the experiments.

## References

1. Yang, V., "Modeling of Supercritical Vaporization, Mixing and Combustion Processes in Liquid-fueled Propulsion System", *Proceeding of the Combustion Institute*, Vol. 28, 2000, pp. 925-942.
2. Fan, X. J., Yu, G., Li, J. G., Zhang, X. Y., and Sung, C. J. Investigation of Vaporized Kerosene Injection and Combustion in a Supersonic Model Combustor. *J. Propulsion Powe*r, 22 (1), 103-110, Jan. – Feb. 2006.
3. Billig, F. S., Dugger, G. L., and Waltrap, P. J., "Inlet-Combustor Interface Problem in Scramjet Engines," *Proceeding of the International Symposium on Air Breathing Engines*, June 1972.
4. Thomas, S. R., Guy, R. W., "Scramjet Testing from Mach 4-20—Present Capability and Needs for the Ninties," *AIAA Paper* 90-1388, June 1990.

5. Vinogradov, V., Grachev, V., Petrov, M., and Sheechman, J., "Experimental Investigation of 2-D Dual Mode Scramjet with Hydrogen Fuel at Mach 4-6," *AIAA Paper* 90-5269, Oct. 1990.
6. Tomioka, S., Murakami, A., Kudo, K., and Mitani, T., "Effects of Injection Configuration on Performance of a Staged Supersonic Combustor," *J. of Propulsion and Power,* Vol. 17, No. 2, March – April 2001.
7. Tomioka, S., Kobayashi, K., Kudo, K., Murakami, A., and Mitani, T., "Combustion Tests of a Staged Supersonic Combustor with a strut," *J. of Propulsion and Power,* Vol. 19, No. 5, Sept. – Oct. 2003.
8. Billig, F. S., Orth, R. C., and Lasky, M., "A Unified Analysis of Gaseous Jet Penetration," *AIAA Journal*, Vol. 9, No. 6, June 1971.

**Table 1 Experimental conditions and measured thrust increments per unit air mass flow rate**

| Fig. | Air | | | Kerosene | | | | Γ, m/s | Injector configuration |
|---|---|---|---|---|---|---|---|---|---|
| | $P_0$, MPa | $T_0$, K | M | $P_f$, MPa | $T_f$, K | $\phi_1$ | $\phi_2$ | | |
| 4 | 1.11 | 1759 | 2.5 | 4.94 | 758 | 1.43 | | 369 | 9 × 1.0 mm |
| | 1.13 | 1765 | 2.5 | 4.95 | 748 | 1.44 | | 312 | |
| | 1.14 | 1820 | 2.5 | 4.90 | 731 | 1.46 | | 312 | |
| | 1.13 | 1837 | 2.5 | 4.96 | 742 | 1.44 | | 343 | |
| 5 | 1.13 | 1749 | 2.5 | 4.18 | 758 | 0.78 | 0.58 | 415 | 9 × 1.0 mm |
| | 1.13 | 1767 | 2.5 | 4.20 | 754 | 0.80 | 0.59 | 381 | |
| | 1.12 | 1778 | 2.5 | 4.32 | 735 | 0.82 | 0.61 | 395 | |
| 6 | 1.13 | 1765 | 2.5 | 4.95 | 748 | 1.42 | | 312 | 9 × 1.0 mm |
| | 1.12 | 1756 | 2.5 | 4.90 | 755 | 1.42 | | 377 | 4 × 1.2 mm |
| | 1.12 | 1672 | 2.5 | 5.86 | 757 | 1.37 | | 450 | 2 × 1.7 mm |
| 7 | 1.12 | 1701 | 2.5 | 4.20 | 753 | 0.58 | 0.79 | 386 | 9 × 1.0 mm |
| | 1.12 | 1712 | 2.5 | 4.00 | 765 | 0.54 | 0.73 | 400 | 4 × 1.2 mm |
| | 1.11 | 1712 | 2.5 | 4.17 | 759 | 0.58 | 0.78 | 377 | 2 × 1.7 mm |
| 8 | 2.45 | 1801 | 3.0 | 4.58 | 755 | 1.05 | | 363 | 9 × 1.0 mm |
| | 2.43 | 1791 | 3.0 | 4.53 | 763 | 1.03 | | 299 | |
| | 2.50 | 1822 | 3.0 | 4.52 | 760 | 1.00 | | 250 | |
| | 2.43 | 1764 | 3.0 | 4.52 | 746 | 1.04 | | 220 | |
| 9 | 2.50 | 1884 | 3.0 | 4.10 | 750 | 0.46 | 0.62 | 344 | 9 × 1.0 mm |
| | 2.38 | 1721 | 3.0 | 4.13 | 761 | 0.45 | 0.61 | 298 | |
| | 2.44 | 1766 | 3.0 | 4.12 | 757 | 0.45 | 0.61 | 296 | |
| 11 | 1.13 | 1711 | 2.5 | 4.22 | 742 | 1.00 | | 371 | 2 × 1.7 mm |
| | 1.13 | 1734 | 2.5 | 5.36 | 763 | 0.98 | | 373 | |
| | 1.12 | 1672 | 2.5 | 5.86 | 757 | 1.37 | | 450 | |